Desalination and Water Treatment
www.deswater.com

doi: 10.5004/dwt.2017.20606

74 (2017) 35–43
May

Numerical study of falling binary liquid film evaporation: liquid film thickness

Abdelaziz Nasr[a,b,*], Abdulmajeed S. Al-Ghamdi[b], M'barek Feddaoui[c], Mohammad S. Alsoufi[b], Sassi Ben Nasrallah[a]

[a]*Laboratory of Thermal and Energy Systems Studies, Monastir University, Ibn Eljazzar Street, 5019 Monastir, Tunisia, Tel. +966 1252 700 70; Fax: +966 1252 700 27; emails: abdelaziz.nasr@ymail.com (A. Nasr), sassi.bennasrallah@yahoo.fr (S. Ben Nasrallah)*
[b]*Mechanical Engineering Department, College of Engineering, Umm Al-Qura University, P.O. Box 5555, Makkah, Saudi Arabia, emails: alghamdi10@hotmail.com (A.S. Al-Ghamdi), mssoufi@uqu.edu.sa (M.S. Alsoufi)*
[c]*Laboratoire Génie de l'Energie, Matériaux et Systèmes (LGEMS), B.P. 1136, ENSA-Agadir, Morocco, email: m.feddaoui@uiz.ac.ma*

Received 7 September 2016; Accepted 17 February 2017

ABSTRACT

A computational study is reported on the combined heat and mass transfer during evaporation of binary liquid film. The binary film is falling down on a vertical channel by mixed convection. The first plate is submitted to a constant heated flux while the other is isothermal and dry. The liquid mixture consists of ethylene glycol and water while the gas mixture is made up of three components: water vapour, ethylene glycol vapour and dry air. The results concern the influence of the operating parameters in the liquid and in the gas on the thickness of the binary liquid film and on the cumulated evaporation rate of binary liquid film.

Keywords: Film thickness; Binary liquid film; Evaporation; Heat and mass transfer; Mixed convection

1. Introduction

The heat and mass transfer during liquid films evaporation in air is important and exists in different industrial applications such as, combustion premixing, drying, industry, desalting, desalination, film cooling and air conditioning. The case of the evaporation of pure liquid has been extensively investigated in many theoretical and experimental studies [1–5]. The case of binary liquid evaporation has also received considerable attention in many studies [6–18]. Khalal et al. [6] presented a numerical study of heat and mass transfer during evaporation of a turbulent binary liquid film. They showed that the heat transferred through the latent mode is more pronounced when the concentration of volatile components is higher in the liquid mixture. Cherif and Daïf [7] numerically analysed the evaporation of binary liquid film flowing on the internal face of the vertical channel. The first plate is wetted and subjected to constant heat flux while the other is insulated and dry. They showed the effect of the mixture composition and film thickness on the coupled heat and mass transfers. Agunaoun et al. [8] reported a numerical investigation of the binary film evaporation flowing on an inclined plate. In fact, they showed the possibility to increase the cumulated evaporation rate of water when the inlet liquid fraction of ethylene glycol is <40%. Palen et al. [9] presented an experimental work of the liquid mixture evaporation inside a vertical tube. They showed that the coefficient of heat transfer between the liquid and the gas can fall of 80% compared with the relative value to the pure water. Hoke and Chen [10] numerically studied the evaporation of a binary liquid film falling on a vertical plate. They presented the evolution of Nusselt and Sherwood numbers. Vijay et al. [11] treated the isotherm evaporation of a binary film. They measured the mass transfer coefficient during the evaporation of a binary film. Baumann and Thiele [12] conducted a study of the binary

* Corresponding author.

film evaporation. El Armouzi [13] and El Armouzi et al. [14] reported a numerical study of the evaporation by mixed convection of a binary liquid film flowing down into two coaxial cylinders. They analysed the effect of the volatilities of the liquid film on the mass and heat transfer. They also showed that the heat and mass transfers are more important near the channel inlet and increase with the wall heat flux density. Saouli et al. [15] studied numerically the evaporation of an Ostwaldian film flowing over an inclined plane surface. They analysed the effect of the behaviour index of the liquid film on the thermal and dynamic characteristics of a liquid–air system. They showed that the behaviour index influences considerably the transfers which are more important for pseudoplastic liquids than for dilatants ones. Cherif et al. [16] presented a comparison between the numerical and experimental study of the evaporation of water film by mixed convection in a vertical channel. They analysed the effect of inlet parameters, in particular of heat flux and air velocity on temperatures in the gas phase and in the film on the evaporation efficiency. Doumenc et al. [17] presented transient Rayleigh–Bénard–Marangoni convection due to cooling by evaporation. They presented numerical results as well as theoretical scalings for the critical parameters for the limiting cases of purely buoyancy-driven and purely surface-tension-driven convection. Machrafi et al. [18] presented a time-dependent Marangoni–Bénard instability of an evaporating binary-liquid layer including gas transients. They developed a good-working analytical model for the description of such delicate transient effects in the gas. Uguz and Narayanan [19] presented the instability in evaporative binary mixtures. They investigated the instability of an evaporating binary mixture underlying its own vapour in an enclosed container. Serpetsi and Yiantsios [20] presented a numerical study of stability characteristics of solutocapillary Marangoni motion in evaporating thin films. They showed that the systems where the surface tension decreases with increasing solute concentration are not immune to instabilities either but there exists a long-wave deformational mode leading to monotonic growth of thickness disturbances.

To the author's knowledge, the previous studies concerned with a numerical analysis of the binary liquid film evaporation along the vertical channel, despite their practical importance, could be useful to be viewed as indicators for wider and more detailed exploration. Thus, the objective of this work is to study the influence of the inlet parameters on the cumulated evaporation rate of binary liquid film and on the liquid film thickness.

2. Analysis

The geometry of the problem under consideration is a vertical parallel plates with channel height H and channel width d (Fig. 1). The right plate is dry and isothermal. The left plate is subjected to a uniform heat flux q_1 and wetted by a binary liquid film (water–ethylene glycol). The liquid film is fed with an inlet liquid temperature $T_{0\ell}$ and liquid mass flow rate at the channel inlet $m_{0\ell}$ The air enters the channel with a temperature $T_{0'}$ a water and ethylene glycol vapour concentrations c_{01} and c_{02} and constant velocity u_0.

2.1. Assumptions

- Vapour mixture is ideal gas.
- The boundary layer approximations are valuable.
- Dufour and Soret effects are negligible.
- Viscous dissipation and radiative heat transfer and pressure work terms are negligible.
- Liquid mixture is ideal.
- Flows and transfers in the two phases are steady, laminar and two-dimensional.

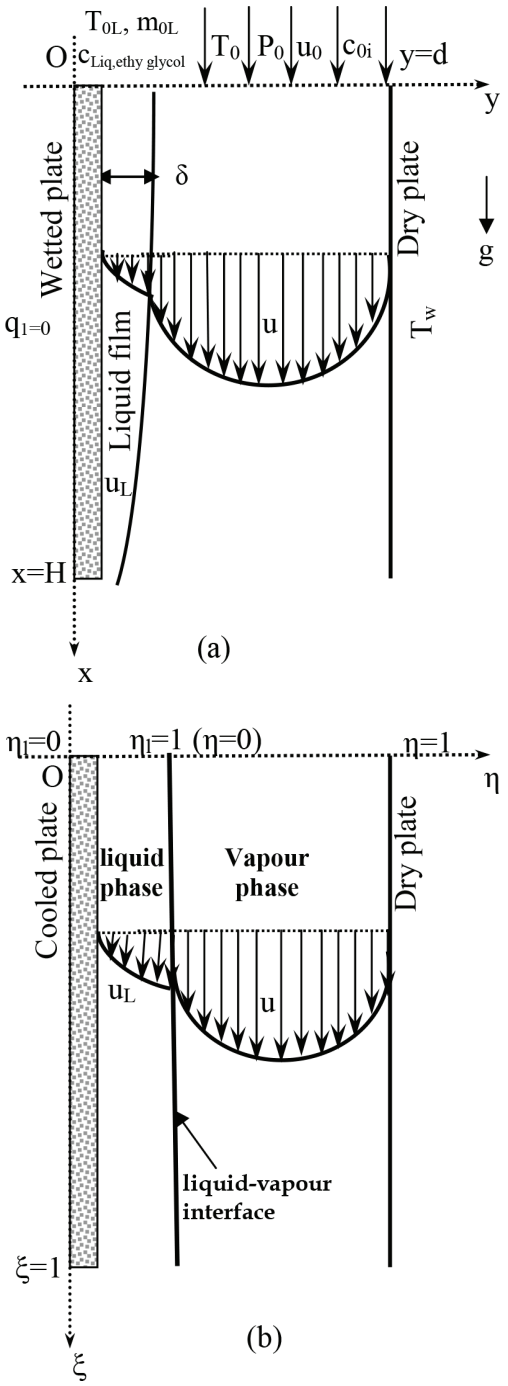

Fig. 1. Physical model.

- The effect of the superficial tension is negligible. The gas–liquid interface is in thermodynamic equilibrium.
- The effect of the wave motion in the liquid film is negligible.

2.2. Governing equations

Following Cherif and Daïf [7], Agunaoun et al. [8], Nasr and Al-Ghamdi [24] and Nasr et al. [25] and in order to fix the position of the liquid–gas interface, we introduce the following transformations (Fig. 1(b)).

In the gaseous phase:

$$\eta = \left(y-\delta\right)/\left(d-\delta\right);\quad \xi = x/H \tag{1}$$

In the liquid phase:

$$\eta_L = y/\delta;\ \xi = x/H \tag{2}$$

Adopting these transformations, the equations governing the flow and heat and mass transfers in the liquid and in the gas phases are as follows [7,8,21–25].

2.2.1. For the liquid phase

Continuity equation:

$$\frac{\partial \rho_\ell u_\ell}{\partial \xi} - \frac{\eta_\ell}{\delta}\frac{\partial \delta}{\partial \xi}\frac{\partial \rho_\ell u_\ell}{\partial \eta_\ell} + \frac{H}{\delta}\frac{\partial \rho_\ell v_\ell}{\partial \eta_\ell} = 0 \tag{3}$$

x-Momentum equation:

$$u_\ell \frac{\partial u_\ell}{\partial \xi} + \left(v_\ell \frac{H}{\delta} - u_\ell \frac{\eta_\ell}{\delta}\frac{\partial \delta}{\partial \xi}\right)\frac{\partial u_\ell}{\partial \eta_\ell} = -\frac{1}{\rho_\ell}\frac{\partial P}{\partial \xi} - \frac{H}{\rho_\ell \delta^2}\frac{\partial}{\partial \eta_\ell}\left(\mu_\ell \frac{\partial u_\ell}{\partial \eta_\ell}\right) + gH \tag{4}$$

Energy equation:

$$u_\ell \frac{\partial T_\ell}{\partial \xi} + \left(v_\ell \frac{H}{\delta} + u_\ell \frac{\eta_\ell - 1}{\delta}\frac{\partial \delta}{\partial \xi}\right)\frac{\partial T_\ell}{\partial \eta_\ell} = \frac{H}{\rho_\ell C_{P\ell}\delta^2}\left\{\frac{\partial}{\partial \eta_\ell}\left(\lambda_\ell \frac{\partial T_\ell}{\partial \eta_\ell}\right) + \rho_\ell D_{\ell,12}\left(c_{p\ell,1} - c_{p\ell,2}\right)\frac{\partial T_\ell}{\partial \eta_\ell}\frac{\partial c_{\ell,1}}{\partial \eta_\ell}\right\} \tag{5}$$

Species diffusion equation:

$$u_\ell \frac{\partial c_{\ell,i}}{\partial \xi} + \left(v_\ell \frac{H}{\delta} + u_\ell \frac{\eta_\ell - 1}{\delta}\frac{\partial \delta}{\partial \xi}\right)\frac{\partial c_{\ell,i}}{\partial \eta_\ell} = \frac{H}{\rho_\ell \delta^2}\frac{\partial}{\partial \eta_\ell}\left(\rho_\ell D_{\ell,12}\frac{\partial c_{\ell,i}}{\partial \eta_\ell}\right),\ i = 1,2 \tag{6}$$

where $c_{\ell,1} + c_{\ell,2} = 1$.

Mass flow rate equation:

$$\int_0^1 \delta \rho_\ell u_\ell d\eta_\ell = \left[m_{0\ell} - H\int_0^\xi \rho v\left(\xi, \eta = 0\right)d\xi\right] \tag{7}$$

2.2.2. For the gaseous phase

The steady two-dimensional laminar flow is governed by the following conservation equations.

Continuity equation:

$$\frac{\partial \rho u}{\partial \xi} - \frac{\eta - 1}{d-\delta}\frac{\partial \delta}{\partial \xi}\frac{\partial \rho u}{\partial \eta} + \frac{H}{d-\delta}\frac{\partial \rho v}{\partial \eta} = 0 \tag{8}$$

x-Momentum equation:

$$u\frac{\partial u}{\partial \xi} + \left(v\frac{H}{d-\delta} + \frac{\eta-1}{d-\delta}\frac{\partial \delta}{\partial \xi}\right)\frac{\partial u}{\partial \eta} = -\frac{1}{\rho}\frac{\partial P}{\partial \xi} - g\beta H\left(T - T_0\right) - g\beta^* H\sum_{i=1}^{2}\left(c_i - c_0\right) - g\beta^* H\sum_{i=1}^{2}\left(c_i - c_0\right) + \frac{1}{\rho}\frac{H}{\left(d-\delta\right)^2}\frac{\partial}{\partial \eta}\left(\mu\frac{\partial u}{\partial \eta}\right) \tag{9}$$

Energy equation:

$$u\frac{\partial T}{\partial \xi} + \left(v\frac{H}{d-\delta} + \frac{\eta-1}{d-\delta}\frac{\partial \delta}{\partial \xi}\right)\frac{\partial T}{\partial \eta} = \frac{H}{\rho C_p\left(d-\delta\right)^2}\left\{\frac{\partial}{\partial \eta}\left(\lambda\frac{\partial T}{\partial \eta}\right) + \rho\sum_{i=1}^{2}\left(D_{g,im}c_{pi} - D_{g,am}c_{pa}\right)\frac{\partial T}{\partial \eta}\frac{\partial c_i}{\partial \eta}\right\} \tag{10}$$

Species diffusion equation:

$$u\frac{\partial c_i}{\partial \xi} + \left(v\frac{H}{d-\delta} + u\frac{\eta-1}{d-\delta}\frac{\partial \delta}{\partial \xi}\right)\frac{\partial c_i}{\partial \eta} = \frac{H}{\rho\left(d-\delta\right)^2}\frac{\partial}{\partial \eta}\left(\rho D_{g,im}\frac{\partial c_i}{\partial \eta}\right),\ i = 1, 2, 3 \tag{11}$$

Mass flow rate equation:

$$\int_0^1 \left(d-\delta\right)\rho u\left(\xi,\eta\right)d\eta = \left[\left(d-\delta_0\right)\rho_0 u_0 + H\int_0^\xi \rho v\left(\xi,\eta=0\right)d\xi\right] \tag{12}$$

2.3. Boundary conditions

For $\xi = 0$ (inlet conditions):

$$T(0,\eta) = T_0;\ c_1(0,\eta) = c_{01};\ c_2(0,\eta) = c_{02};\ u(0,\eta) = u_0;\ P = P_0 \tag{13}$$

$$T_\ell\left(0,\eta_\ell\right) = T_{0\ell};\ \delta\left(0\right) = \delta_0;\ \int_0^1 \rho_{0\ell}\delta_0 u_\ell\left(0,\eta_\ell\right)d\eta_\ell = m_{0\ell};\ c_{\ell i}\left(0,\eta_\ell\right) = c_{0\ell i} \tag{14}$$

At $\eta = 1$ (dry plate):

$$u\left(\xi,1\right) = 0;\ v\left(\xi,1\right) = 0;\ T\left(\xi,1\right) = T_w;\ \left(\frac{\partial c_i}{\partial \eta}\right)_{\eta=1} = 0 \tag{15}$$

At $\eta_\ell = 0$ (wet plate):

$$u_\ell\left(\xi,0\right) = 0;\ v_\ell(\xi,0) = 0;\ q_1 = -\lambda_\ell\frac{1}{\delta}\left(\frac{\partial T_\ell}{\partial \eta_\ell}\right)_{\eta_\ell=0};\ \left(\frac{\partial c_{\ell i}}{\partial \eta_\ell}\right)_{\eta_\ell=0} = 0 \tag{16}$$

At η = 0 (η_ℓ = 1) (gas–liquid interface):
The continuities of the velocities and temperatures give:

$$u_\ell\left(\xi,\eta_\ell=1\right)=u\left(\xi,\eta=0\right);\ T_\ell\left(\xi,\eta_\ell=1\right)=T\left(\xi,\eta=0\right) \tag{17}$$

The energy balance at the interface is given by the equation:

$$-\frac{1}{\delta}\lambda_\ell\left(\frac{\partial T_\ell}{\partial\eta_\ell}\right)_{\eta_\ell=1}=-\frac{1}{d-\delta}\lambda\left(\frac{\partial T}{\partial\eta}\right)_{\eta=0}+\dot{m}L_v \tag{18}$$

$$\text{with } \dot{m}=-\frac{\rho\sum_{i=1}^{2}D_{g,im}\left(\frac{\partial c_i}{\partial\eta}\right)_{\eta=0}}{\left(d-\delta\right)\left(1-\sum_{i=1}^{2}c_i\left(\xi,\eta=0\right)\right)} \text{ and } L_v=\sum_{i=1}^{2}w_{\ell i}L_{vi}.$$

The concentration of species *i* vapour can be evaluated by:

$$c_1\left(\xi,\eta=0\right)=-\frac{p^*_{vs,1}}{p^*_{vs,1}+\left[p^*_{vs,2}\frac{M_2}{M_1}\right]+\left[p-p^*_{vs,1}-p^*_{vs,2}\right]\frac{M_a}{M_1}} \tag{19}$$

The transverse velocity component of the mixture at the interface is obtained by assuming the interface to be semipermeable:

$$v\left(\xi,\eta=0\right)=-\frac{\frac{1}{d-\delta}\sum_{i=1}^{2}D_{g,im}\left(\frac{\partial c_i}{\partial\eta}\right)_{\eta=0}}{1-\sum_{i=1}^{2}c_i\left(\xi,\eta=0\right)} \tag{20}$$

The continuities of shear stress and local evaporated mass flux of species *i* give:

$$\frac{1}{\delta}\mu_\ell\left(\frac{\partial u_\ell}{\partial\eta_\ell}\right)_{\eta_\ell=1}=\frac{1}{d-\delta}\mu\left(\frac{\partial u}{\partial\eta}\right)_{\eta=0} \tag{21}$$

$$\dot{m}_i=\dot{m}c_{\ell i}-\frac{\rho_\ell D_{\ell,im}}{\delta}\left(\frac{\partial c_{\ell i}}{\partial\eta_\ell}\right)_{\eta_\ell=1}=\dot{m}c_i-\frac{\rho D_{g,im}}{d-\delta}\left(\frac{\partial c_i}{\partial\eta}\right)_{\eta=0} \tag{22}$$

3. Solution method

To check the adequacy of the numerical scheme adopted in the present study, the procedure has been tested by comparing the present solutions for the total evaporating rate (M_r) and the interfacial temperature ($T_w - T_0$) with the results of Cherif and Daïf [7] for the case of the evaporation of the binary liquid film (Figs. 2(a) and (b)). The comparison has been made for T_0 = 293.15 K, c_{01} = 0, c_{02} = 0, $T_{0\ell}$ = 293.15 K, q_2 = 0, $m_{0\ell}$ = 0.02 kg m^{-1} s^{-1}, Re = 1,000, the geometrical ratio is d/H = 0.015, the imposed wall heat flux is q_1 = 3,000 W m^{-2} and the inlet film composition of ethylene glycol is $c_{\ell i,\text{ ethylene glycol}}$ = 0.5. Figs. 2(a) and (b) show a satisfactory conformity between our results and those obtained by Cherif and Daïf [7].

4. Results and discussions

All the results have been obtained for the case of T_w = 293.15 K and the geometrical ratio is d/H = 0.015. The effects of the inlet liquid concentration of ethylene glycol c_{liq} on the liquid film thickness and cumulated evaporation rate are, respectively, illustrated in Figs. 3(a) and (b). It is shown from Fig. 3(a) that the liquid film thickness δ(x) increases with an increase of the inlet liquid concentration of ethylene glycol $c_{\text{liq, ethylene glycol}}$. It is generally obvious that when the inlet liquid concentration of ethylene glycol (the less volatile component) increases the mixture evaporation rate M_r decreases. This result tends to increase the film thickness δ(x). In accordance with the previous results, an increase of the inlet liquid concentration of ethylene glycol (the more viscous) increases the viscosity of the liquid

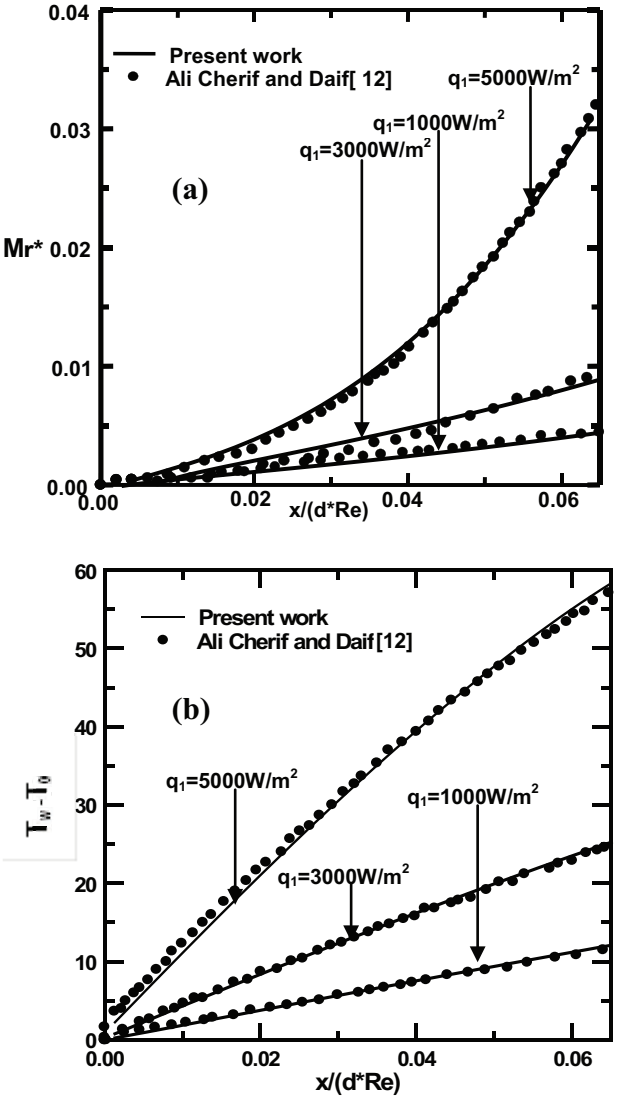

Fig. 2. Comparison of present work with these of Cherif and Daïf [7] with $c_{\text{liq, ethylene glycol}}$ = $c_{\text{liq, water}}$ = 0.5 (50% water–ethylene glycol mixture): (a) validation of calculated total evaporating rate along the channel and (b) validation of calculated interfacial temperature along the channel.

mixture leading to an increase of the liquid film thickness $\delta(x)$. It can be noted from Fig. 3(b) that the cumulated evaporation rate of binary liquid film M_r decreases with an increase of the film composition of ethylene glycol. This result can be explained by the fact that when we increase the inlet liquid concentration of ethylene glycol, the volatility of the liquid mixture decreases (the ethylene glycol is less volatile than the water), consequently the mixture evaporation decreases. Figs. 4(a) and (b) present, respectively, the axial evolution of liquid film thickness and the total accumulated evaporation rate for different inlet liquid mass flow $m_{0\ell}$. It is observed from Fig. 4(a) that the liquid film thickness along the channel $\delta(x)$ increases with an increase of the inlet liquid mass flow $m_{0\ell}$. Whereas Fig. 4(b) shows that a decrease of the inlet liquid mass flow causes a greater mixture evaporation rate M_r. In fact, an increase of the inlet liquid flow enhances the cooling at the interface and consequently reduces the liquid mixture evaporation. Figs. 5(a) and (b) show that an increase of the inlet liquid temperature enhances the mixture evaporation M_r and consequently reduces the liquid film thickness $\delta(x)$ along the channel. Fig. 6(b) presents the impact of the inlet gas temperature T_0 on the cumulated evaporation

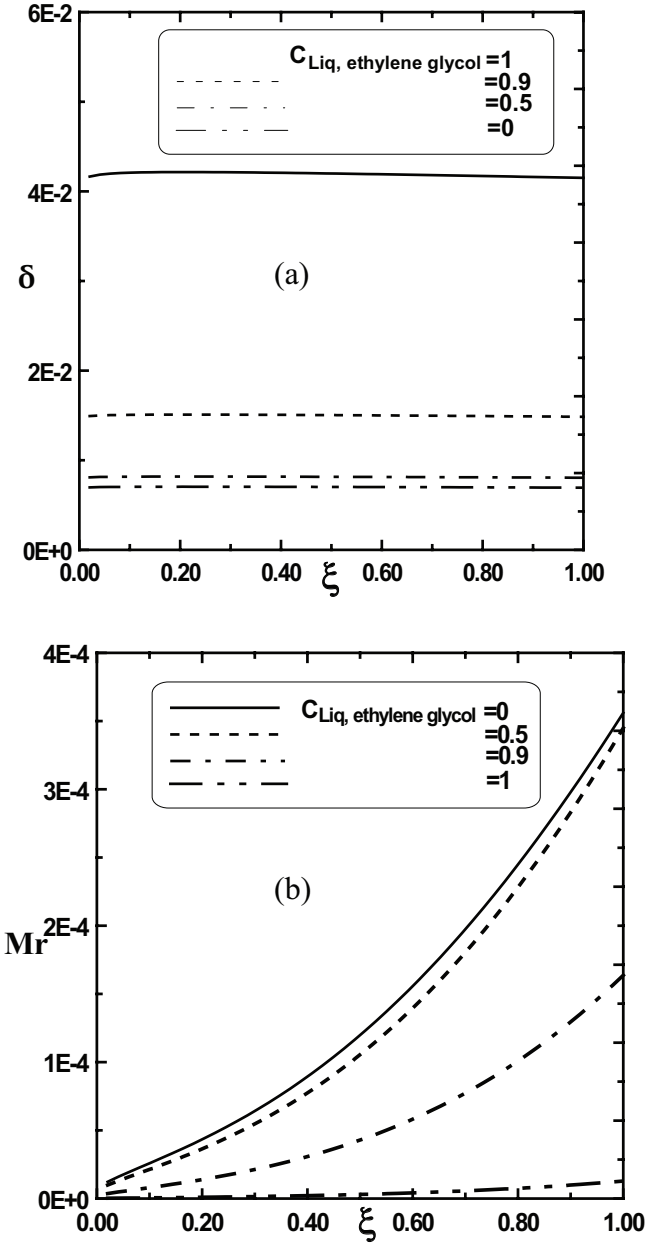

Fig. 3. The evolution of: (a) liquid film thickness and (b) total cumulated evaporation rate of liquid mixture, along the channel with different values of the inlet film composition in the adiabatic case: $c_{01} = 0$, $c_{02} = 0$, $T_0 = 20°C$, $u_0 = 1$ m s^{-1}, $T_{0\ell} = 20°C$, $m_{0\ell} = 0.015$ kg m^{-1} s^{-1}, $q_1 = 3{,}000$ W m^{-2}.

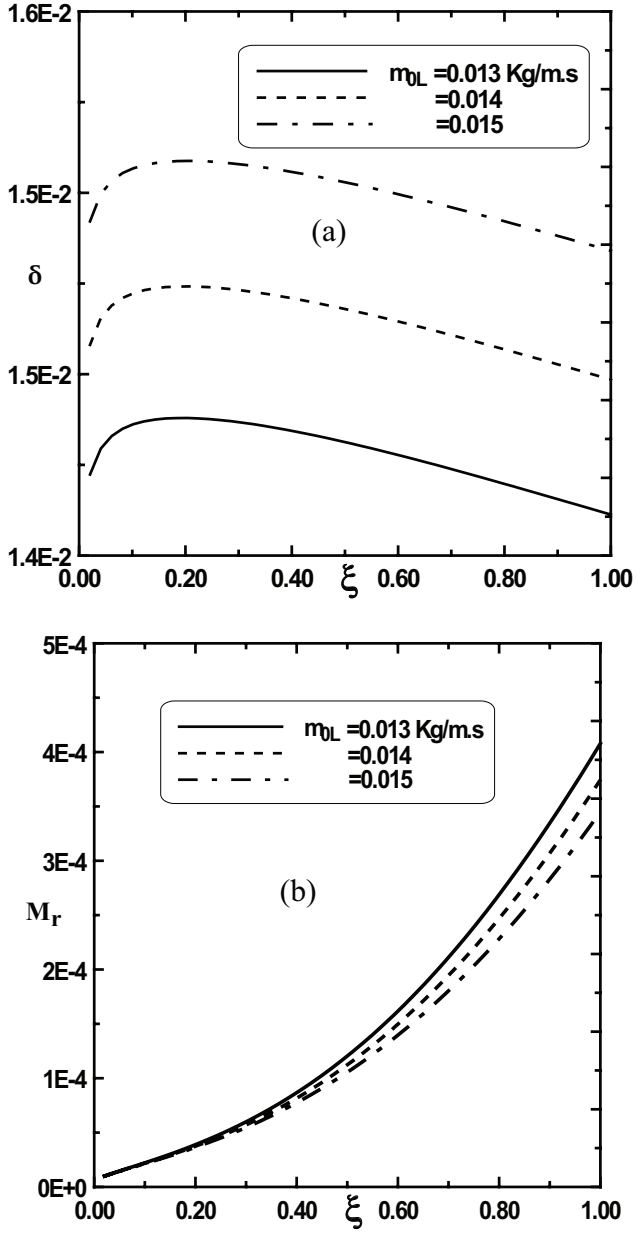

Fig. 4. The evolution of: (a) liquid film thickness and (b) total cumulated evaporation rate of liquid mixture, along the channel with different values of the inlet liquid mass flow: $c_{01} = 0$, $c_{02} = 0$, $T_0 = 20°C$, $u_0 = 1$ m s^{-1}, $T_{0\ell} = 20°C$, $c_{\text{liq, ethylene glycol}} = c_{\text{liq, water}} = 0.5$, $q_1 = 3{,}000$ W m^{-2}.

rate of liquid mixture M_r. An analysis of the results deduced from this figure shows that an increase of the inlet gas temperature T_0 enhances the evaporation of liquid mixture. Consequently, the liquid film thickness along the channel $\delta(x)$ decreases (Fig. 6(a)). Fig. 7(a) indicates that the liquid film thickness along the channel $\delta(x)$ decreases with an increase of the external heat flux q_1. This result can be justified by the fact that the increase of the external heat flux q_1 enhances the mixture evaporation (Fig. 7(b)) causing a decrease of the liquid film thickness along the channel $\delta(x)$. Now, we turn our attention to improve the understanding of the effect of the inlet concentration of water vapour c_{01} on the mixture evaporation and on the liquid film thickness $\delta(x)$. In Fig. 8(b), we can observe that a decrease of the inlet concentration of water vapour c_{01} causes greater liquid mixture evaporation and consequently a smaller liquid film thickness $\delta(x)$ along the channel (Fig. 8(a)).

5. Conclusion

The binary film evaporation along a vertical channel by mixed convection has been numerically studied. The binary liquid film (water–ethylene glycol) flows down on one heated plate of a vertical channel. The second plate is dry and isothermal. The effect of the inlet parameters on the liquid film thickness $\delta(x)$ and on the total cumulated evaporation rate of liquid mixture M_r is analysed. The major results are briefly summarised in the following:

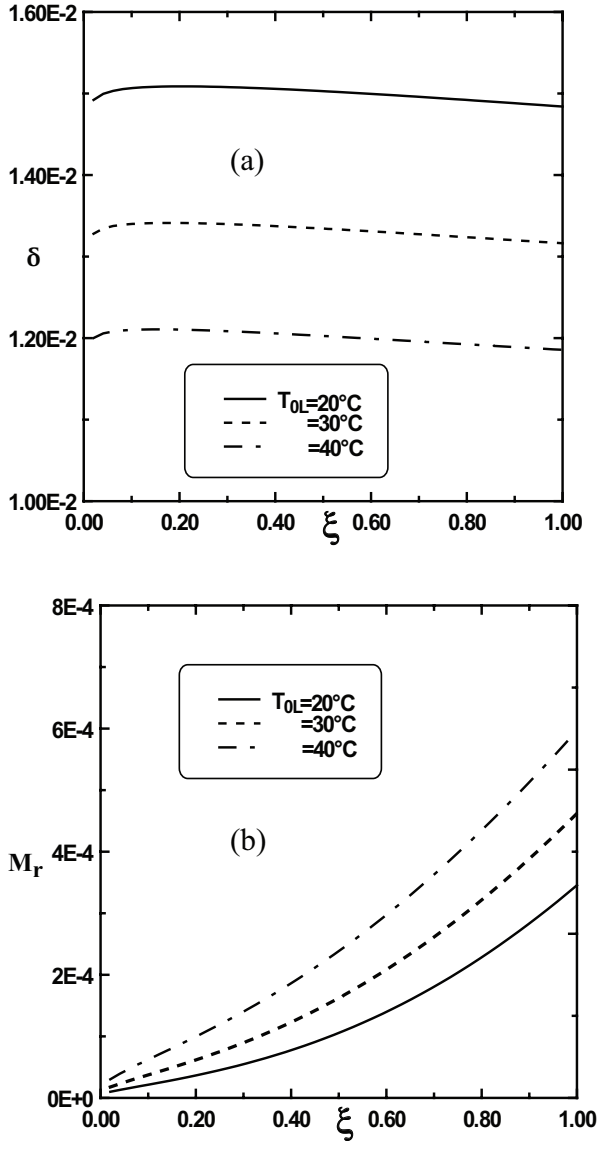

Fig. 5. The evolution of: (a) liquid film thickness and (b) total cumulated evaporation rate of liquid mixture, along the channel with different values of the inlet liquid temperature: $c_{01} = 0$, $c_{02} = 0$, $T_0 = 20°C$, $u_0 = 1$ m s^{-1}, $m_{0\ell} = 0.015$ kg m^{-1} s^{-1}, $c_{\text{liq, ethylene glycol}} = c_{\text{liq, water}} = 0.5$, $q_1 = 3{,}000$ W m^{-2}.

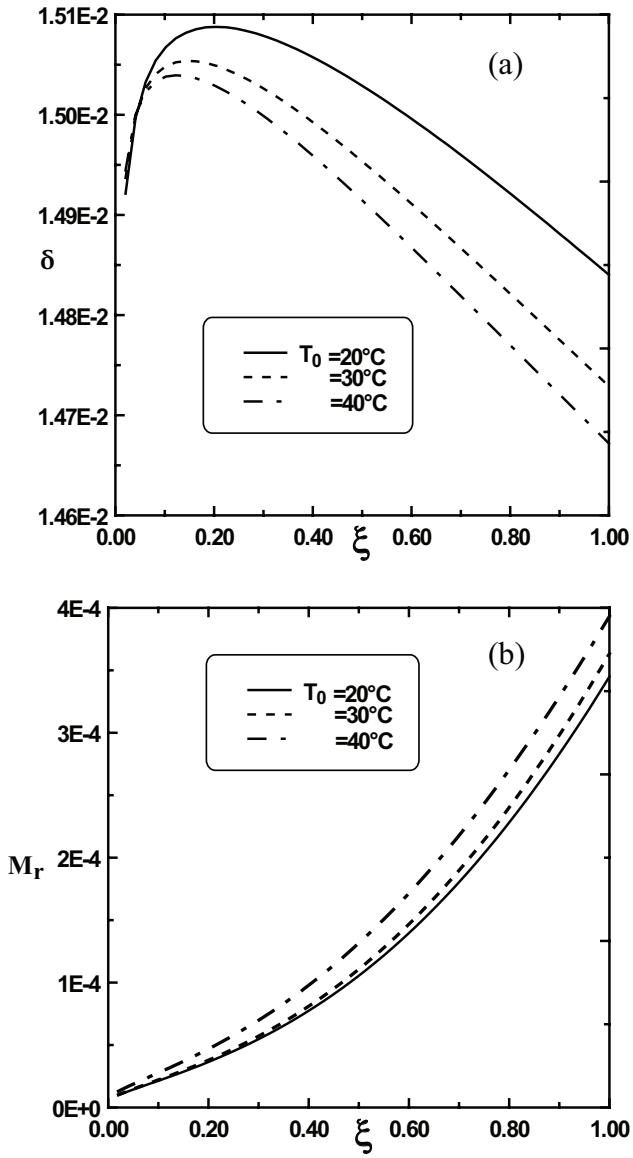

Fig. 6. The evolution of: (a) liquid film thickness and (b) total cumulated evaporation rate of liquid mixture, along the channel with different values of the inlet gas temperature: $c_{01} = 0$, $c_{02} = 0$, $u_0 = 1$ m s^{-1}, $T_{0\ell} = 20°C$, $m_{0\ell} = 0.015$ kg m^{-1} s^{-1}, $c_{\text{liq, ethylene glycol}} = c_{\text{liq, water}} = 0.5$, $q_1 = 3{,}000$ W m^{-2}.

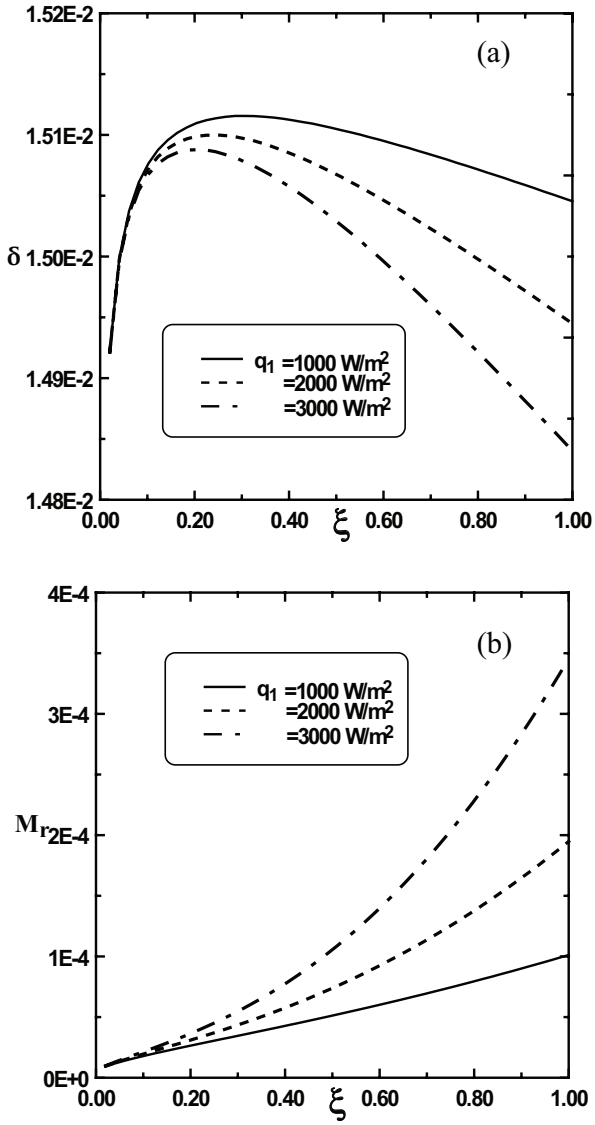

Fig. 7. The evolution of: (a) liquid film thickness and (b) total cumulated evaporation rate of liquid mixture, along the channel with different values of external heat flux: c_{01} = 0, c_{02} = 0, T_0 = 20°C, u_0 = 1 m s^{-1}, $T_{0\ell}$ = 20°C, $m_{0\ell}$ = 0.015 kg m^{-1} s^{-1}, $c_{\text{liq, ethylene glycol}}$ = $c_{\text{liq, water}}$ = 0.5.

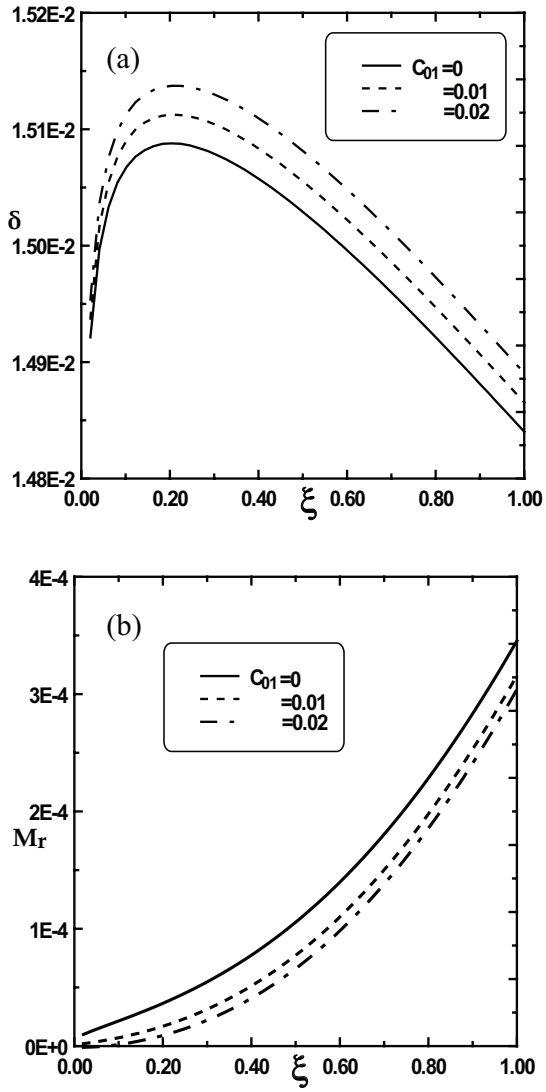

Fig. 8. The evolution of: (a) liquid film thickness and (b) total cumulated evaporation rate of liquid mixture, along the channel with different values of ambient concentration of water vapour: c_{02} = 0, T_0 = 20°C, u_0 = 1 m s^{-1}, $T_{0\ell}$ = 20°C, $m_{0\ell}$ = 0.015 kg m^{-1} s^{-1}, $c_{\text{liq, ethylene glycol}}$ = $c_{\text{liq, water}}$ = 0.5, q_1 = 3,000 W m^{-2}.

- An increase of the inlet liquid concentration of ethylene glycol $c_{\text{liq, ethylene glycol}}$, the ambient concentration of water vapour c_{01} and the inlet liquid mass flow $m_{0\ell}$ induces an increase of the liquid film thickness $\delta(x)$.
- An increase of the inlet liquid temperature $T_{0\ell}$, the inlet gas temperature T_0 and the external heat flux q_1, induces a decrease in the liquid film thickness $\delta(x)$ along the channel.
- A decrease of the inlet liquid concentration of ethylene glycol $c_{\text{liq, ethylene glycol}}$, the ambient concentration of water vapour c_{01} and the inlet liquid mass flow $m_{0\ell}$ benefits the mixture evaporation.
- An increase of the inlet liquid temperature $T_{0\ell}$, the inlet gas temperature T_0 and the external heat flux q_1, enhances the mixture evaporation.

Symbols

c_i	—	Mass fraction for species *i* vapour
c_{0i}	—	Mass fraction for species *i* vapour in the inlet condition
$c_{\ell i}$	—	Mass fraction for species *i* in the liquid film ($c_{\ell 1} + c_{\ell 2} = 1$)
$c_{\text{liq, ethylene glycol}}$	—	Inlet liquid concentration (composition or mass fraction) of ethylene glycol in the liquid mixture ($c_{\text{liq, ethylene glycol}} = 1 - c_{\text{liq, water}}$)
c_p	—	Specific heat at constant pressure, J kg^{-1} K^{-1}
c_{pa}	—	Specific heat for air, J kg^{-1} K^{-1}
c_{pvi}	—	Specific heat for species *i* vapour, J kg^{-1} K^{-1}
d	—	Channel width, m
$D_{g, im}$	—	Mass diffusivity of species *i* vapour in the gas mixture, m^2 s^{-1}

$D_{g,am}$ — Mass diffusivity of dry air in the gas mixture, $m^2 s^{-1}$
D_L — Mass diffusivity of species *i* in the liquid film mixture, $m^2 s^{-1}$
H — Channel length, m
I — Grid point index number in the flow direction
J — Grid point index number in transverse direction
L_v — Latent heat of evaporation of mixture, $J kg^{-1}$
L_{vi} — Latent heat of evaporation of species *i*, $J kg^{-1}$
— Local evaporation rate of species *i*, $kg s^{-1} m^{-2}$
$\dot{m}$ — Local evaporation rate of mixture ($\dot{m} = \dot{m}_1 + \dot{m}_2$), $kg s^{-1} m^{-2}$
$m_{0\ell}$ — Inlet liquid flow rate, $kg s^{-1}$
M_r — Total evaporation rate of mixture $\left(Mr = \int_0^{\xi} \dot{m}(\xi) d\xi \right) \left[\text{kg.s}^{-1}.\dot{\text{m}}^{-1} \right]$
M_r^* — Total evaporation rate of mixture given by Cherif and Daïf [7] ($Mr^* = M_r/0.004$)
p — Pressure in the channel, $N m^{-2}$
p_{vsi} — Pressure of saturated vapour of species *i*, $N m^{-2}$
p_{vsi}^* — Partial pressure of species *i* at the interface liquid–vapour, $N m^{-2}$
p_{vsm} — Pressure of mixture vapour at the interface liquid–vapour ($p^*_{vs1} + p^*_{vs2}$), $N m^{-2}$
$c_{0\ell i}$ — Inlet mass fraction for species *i* in the liquid film ($c_{0\ell 1} = c_{\text{liq, water}}$ and $c_{0\ell 2} = c_{\text{liq, ethylene glycol}}$)
T — Absolute temperature, K
T_s — Interface temperature, K
T_w — Dry wall temperature, K
T_p — Wetted wall temperature, K
q_1 — External heat flux of wetted wall, $W m^{-2}$
g — Gravitational acceleration, $m s^{-2}$
Re — Reynolds number ($Re = u_0 d/n_0$)
u — Axial velocity, $m s^{-1}$
v — Transverse velocity, $m s^{-1}$
x — Coordinate in the axial direction, m
y — Coordinate in the transverse direction, m

Greek

λ — Thermal conductivity of the fluid, $W m^{-1} K^{-1}$
μ — Dynamic viscosity of the fluid, $kg m^{-1} s^{-1}$
ν — Kinematic viscosity of the fluid, $m^2 s^{-1}$
ρ — Density of the gas, $kg m^{-3}$
η — Dimensionless coordinate in the transverse direction
ξ — Dimensionless coordinate in the flow direction
δ — Liquid film thickness, m
β — Thermal expansion coefficient $-1/\rho(\partial\rho/\partial T)_{p,c}$, K^{-1}
b* — Mass expansion coefficient $-1/\varrho(\partial\varrho/\partial c)_{p,T}$

Subscripts

i — Species *i* (1 for water vapour, 2 for ethylene glycol vapour and 3 for dry air)
0 — Inlet condition
L — Liquid phase
a — Dry air
m — Mixture
s — Interface
am — Dry air in the mixture
im — Species *i* in the mixture
Li — Species *i* in the liquid

References

[1] W.M. Yan, Evaporative cooling of liquid film in turbulent mixed convection channel flows, Int. J. Heat Mass Transfer, 41 (1998) 3719–3729.
[2] M. Oubella, M. Feddaoui, R. Mir, Numerical study of heat and mass transfer during evaporation of a thin liquid film, Therm. Sci., 19 (2015) 1805–1819. doi: 10.2298/TSCI130128145O.
[3] M. Feddaoui, E. Belahmidi, A. Mir, A. Bendou, Numerical study of the evaporative cooling of liquid film in laminar mixed convection tube flows, Int. J. Therm. Sci., 40 (2001) 1011–1020.
[4] C. Debbissi, J. Orfi, S. Ben Nasrallah, Evaporation of water by free convection in a vertical channel including effects of wall radiative properties, Int. J. Heat Mass Transf., 44 (2001) 811–826.
[5] M. Feddaoui, A. Mir, E. Belahmidi, Co-current turbulent mixed convection heat and mass transfer in falling film of water inside a vertical heated tube, Int. J. Heat Mass Transf., 46 (2003) 3497–3509.
[6] L. Khalal, M. Feddaoui, T. Mediouni, Numerical study of heat and mass transfer during evaporation of a turbulent binary liquid film, Therm. Sci., 19 (2013) 25. doi: 10.2298/TSCI120927025K.
[7] A. Cherif, A. Daïf, Numerical study of heat and mass transfer in mixed convection inside a vertical channel with a binary liquid film streaming in one of its heated walls., Int. J. Heat Mass Transf., 42 (1999) 2399–2418.
[8] A. Agunaoun, A. Il Idrissi, A. Daif, R. Barriol, study of the evaporation in mixed convection of a liquid film of a binary mixture flowing on an inclined plane subjected to a constant heat flux, Int. J. Heat Mass Transf., 41 (1998) 2197–2210.
[9] J.W. Palen, Q. Wang, J.C. Chen, Falling film evaporation of binary mixtures, AIChE J., 40 (1994) 207–214.
[10] B.C. Hoke Jr., J.C. Chen, Mass transfer in evaporating falling liquid film mixtures, AIChE J., 38 (1992) 781–787.
[11] R. Vijay, Mhetar, J.C. Slattery, The Stefan problem of a binary liquid mixture, Chem. Eng. Sci., 52 (1997) 1237–1242.
[12] W.W. Baumann, F. Thiele, Heat and mass transfer in evaporating two-component liquid film flow, Int. J. Heat Mass Transf., 33 (1990) 267–273.
[13] M. El Armouzi, Numerical study of evaporation by mixed convection of a binary liquid film flowing down the wall of two coaxial cylinders, Thesis of Perpignan University, 2000.
[14] M. El Armouzi, X. Chesneau, B. Zeghmati, Numerical study of evaporation by mixed convection of a binary liquid film flowing down the wall of two coaxial cylinders, Heat Mass Transf., 41 (2005) 375–386.
[15] S. Saouli, M. Boumaza, M. Daguenet, Evaporation in forced convection of an Ostwaldian permanent laminar film flowing over an isothermal inclined plane surface, Int. J. Therm. Sci., 42 (2003) 1115–1128.
[16] A.S. Cherif, M.A. Kassim, B. Benhamou, S. Harmand, J.P. Corriou, S. Ben Jabrallah, Experimental and numerical study of mixed convection heat and mass transfer in a vertical channel with film evaporation, Int. J. Therm. Sci., 50 (2011) 942–953.

[17] F. Doumenc, T. Boeck, B. Guerrier, M. Rossi, Transient Rayleigh-Benard-Marangoni convection due to evaporation: a linear non-normal stability analysis, J. Fluid Mech., 648 (2010) 521–539.
[18] H. Machrafi, A. Rednikov, P. Colinet, P.C. Dauby, Time-dependent Marangoni-Bénard instability of an evaporating binary-liquid layer including gas transients, Phys. Fluids, 25 (2013) 084106.
[19] K.E. Uguz, R. Narayanan, Instability in evaporative binary mixtures. I. The effect of solutal Marangoni convection, Phys. Fluids, 24 (2012) 094101.
[20] S.K. Serpetsi, S.G. Yiantsios, Stability characteristics of solutocapillary Marangoni motion in evaporating thin films, Phys. Fluids, 24 (2012) 122104.
[21] R.C. Reid, T.K. Sherwood, The Properties of Gases and Liquids, McGraw-Hill, New York, 1958.
[22] R.B. Bird, W.E. Stewart, E.N. Lightfoot, Transport Phenomena, Wiley, New York, 1960.
[23] A. Missenard, conductivity of solids, liquids and of gas, Edition Eyrolles, Paris, 1965.
[24] A. Nasr, A.S. Al-Ghamdi, Numerical study of evaporation of falling liquid film on one of two vertical plates covered with a thin porous layer by free convection, Int. J. Therm. Sci., 112 (2017) 335–344.
[25] A. Nasr, C. Debbissi Hfaiedh, S. Ben Nasrallah, Numerical study of evaporation by mixed convection of a binary liquid film, Energy, 36 (2011) 2316–2327.